THERMAL ANALYSIS IN FIRE-RESISTANCE FURNACE

Piloto, P.A.G. [1], Mesquita, L.M.R. [1]; Alexandre Pereira [2]

[1]- Applied Mech. Dep., Polytechnic Inst. of Bragança, Campus Sta. Apolónia,
5301-857 Bragança, Portugal

[2]- Fellow research, Polytechnic Inst. of Bragança, Campus Sta. Apolónia,
5301-857 Bragança, Portugal

ABSTRACT

Fire resistance rating of building construction elements is defined under fire-resistance test furnace. The geometry and shape of fire-resistance furnaces is not defined by any prescriptive document, being necessary to comply thermally with specified nominal fire curves, such as ISO 834 or hydrocarbon [1,2].

This research work intends to measure temperatures inside furnace volume, using sixteen plate thermocouples to compare average temperature in four planes. Those planes are compared with reference thermocouple which is responsible for controlling furnace operation, see figure 1. Three tests were performed, the first two running with ISO 834, during 45 minutes and the last one running with hydrocarbon curve, during 30 minutes. Experimental results demonstrate that relative temperature differences are smaller than 30 % in the initial test stage, being smaller than 5 %, after 500 [s] until the end of the tests.

The numerical simulations were performed using Fluent CFD, using the structured finite volume mesh method. The Eddy Dissipation Model (EDM) was used for chemical species transport and reacting flow. The governing equations for mass, momentum and energy were solved for the three dimensional unsteady incompressible flow, with radiative heat transfer and turbulence model. The numerical results agree well with experimental results, being the relative temperature difference smaller than 5% for each nominal test. Numerical simulation also reveals the localized effect of each burner.

1 INTRODUCTION

The thermal performance of fire-resistance furnace is investigated. Furnace environment is normally considered homogeneous and with uniform temperature distribution, following specified nominal temperature evolution. Tests were conducted at the Polytechnic Institute of Bragança laboratory (LERM) using the 1 cubic meter fire-resistance furnace. This small furnace is suitable for initial validation of experimental temperature measurements. The furnace has 4 propane burners with 90 [kW] maximum power each, reference Kromschröder BIO 65 HM-100/35-72/8. This furnace complies with European Standard EN 1363-1, considering the maximum deviation between reference temperature and the theoretical specified nominal curve for temperature.

Four planes were defined to evaluate the furnace temperature performance. Four plate thermocouples define each plane. Plane X150 and X850 are parallel to the exhaust zone while plane Z150 and Z850 are parallel to the transversal plane of burners.

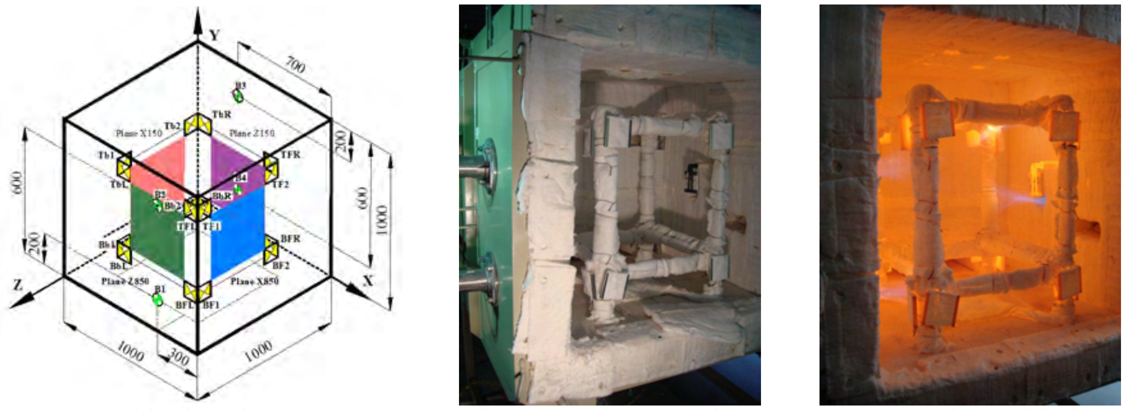

a) Furnace model with four burners Bi (i=1,4).
b) Geometric position for plate thermocouples inside furnace.
c) Furnace with opened door after running test 3.

Fig.1. Model for fire-resistance furnace.

Three tests were performed. The first two tests used ISO834 nominal fire curve, defined by equation (1), while the last one used hydrocarbon nominal fire curve (2). In these equations, θ_g represents reference furnace temperature for time t, during testing conditions.

$$\theta_g = 20 + 345 \times \log_{10}(8 \times t + 1) \quad \left[\theta_g (^\circ C); t(\min)\right] \tag{1}$$

$$\theta_g = 20 + 1080 \times \left(1 - 0,325 \times e^{-0,167t} - 0,675 \times e^{-2,5t}\right) \quad \left[\theta_g (^\circ C); t(\min)\right] \tag{2}$$

The thermal performance is determined by the comparison between average plane temperatures with reference furnace temperature, which represents each nominal fire curve. Numerical simulations are also performed, using computational fluid dynamics, to evaluate thermal performance and validate experimental tests.

2 EXPERIMENTAL TESTS

The fire-resistance furnace was instrumented with 16 plate thermocouples, suspended at insulated slenderness steel frame, see figure 2. Plate thermocouples fulfil standards and were positioned according to the vertex position of 700 [mm^2] cube, centered inside furnace.

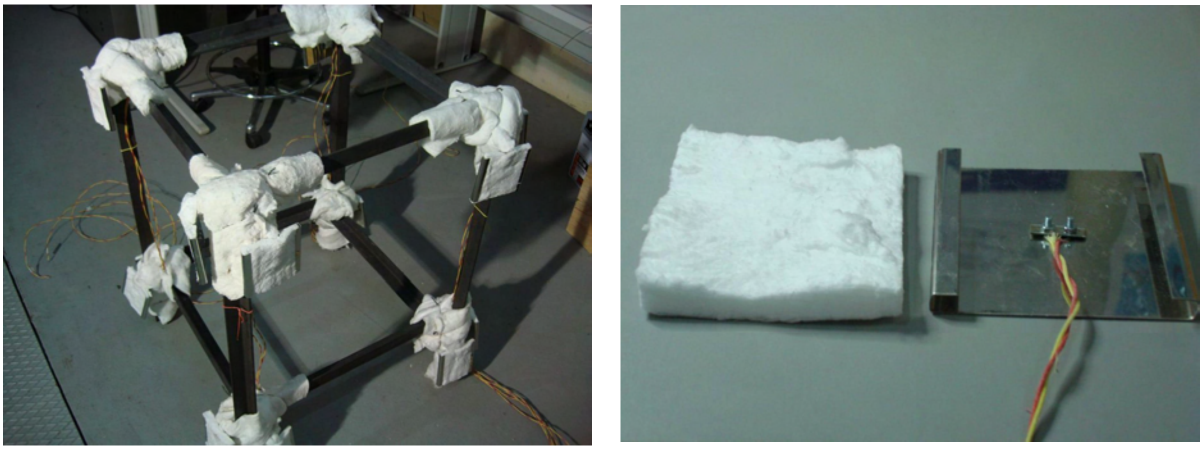

a) Relative position for plate thermocouples.
b) Plate thermocouple (type K and stainless steel plate A304).

Fig.2. Plate thermocouple instrumentation.

Thermocouple control is achieved by matching the measured thermocouple temperature with the prescribed nominal fire curve. However, since thermocouples irradiate heat, they adjust themselves to the temperature at which there is a balance between the convection and net radiative heat transfer, [3]. Plate thermocouple is a stainless steel plate with 100 [mm^2] and 0.7 ± 0.1 [mm] thick. The emissivity was considered greater than 0.7. The wire thermocouple is positioned on the back face, screwed with a small plate and insulated with ceramic fibre, [1].

Measurements were performed with multi-channel data acquisition system, MGCplus from HBM, with frequency equal to 0.1 [Hz]. Results were averaged from 4 plate thermocouples for each plane. Plane X850 was defined by the average temperature readings on TF1, TF2, BF1, BF2, Plane X150 was defined by the average temperature readings on Tb1, Tb2, Bb1, Bb2, Plane Z850 was defined by the average temperature readings on TFL, BFL, TbL, BbL, while Plane Z150 was defined by the average temperature readings on TbR, TFR, BbR and BFR.

Figure 3 represents each measured temperature with plate thermocouple and the reference temperature for furnace.

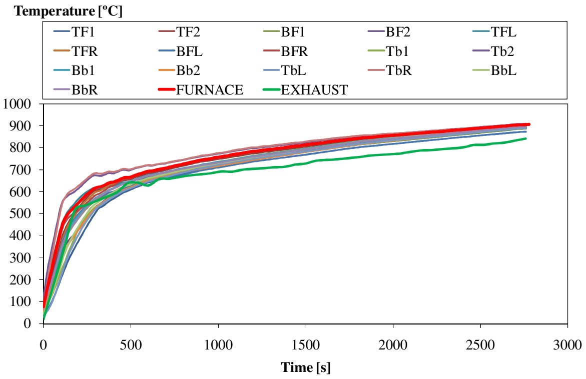

a) *Test 1 with ISO 834 nominal curve.*

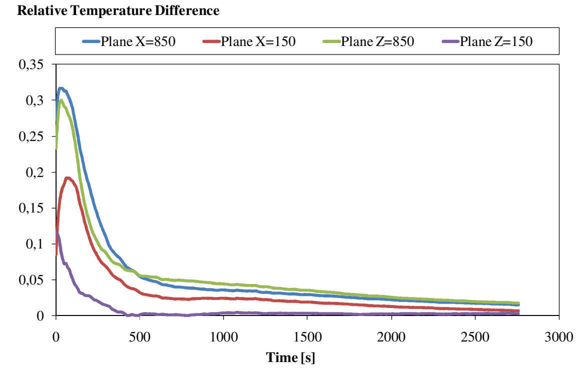

b) *Test 1 with ISO 834 nominal curve.*

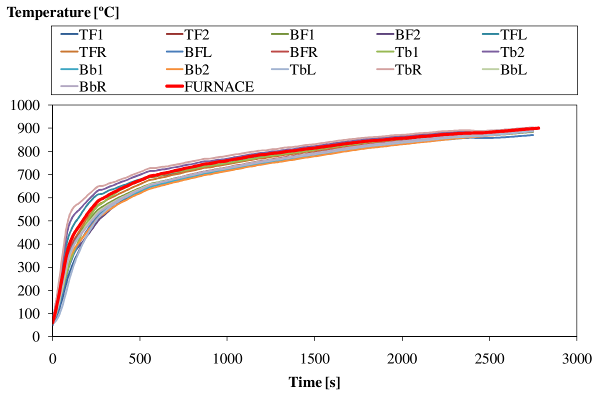

c) *Test 2 with ISO 834 nominal curve.*

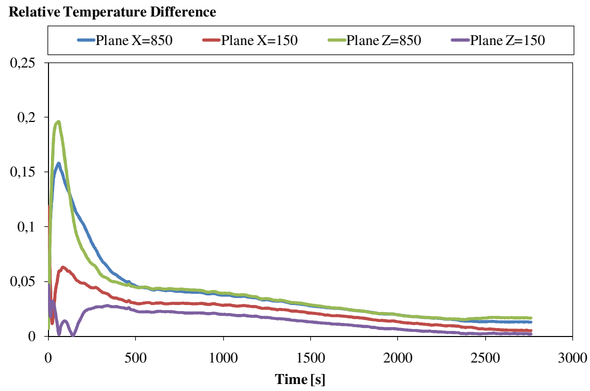

d) *Test 2 with ISO 834 nominal curve.*

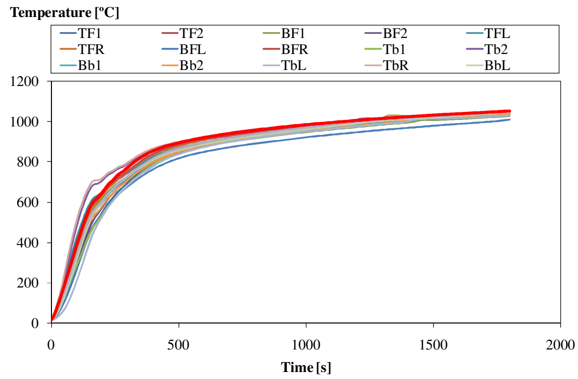

e) Test 3 with hydrocarbon nominal curve.

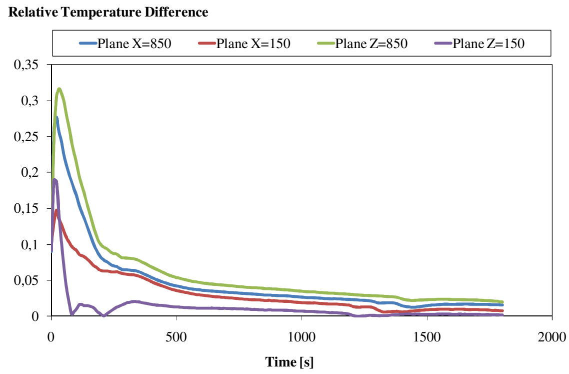

f) Test 3 with hydrocarbon nominal curve.

Fig.2. Experimental results for temperature measurements and relative temperature deviations for each plane.

The relative difference between each average plane temperature and reference temperature from furnace is below 5%, after the initial testing phase, corresponding to 500 [s]. Higher relative difference is expected before, due to higher temperature variation with time.
The exhaust temperature was also measured for test 1. There was a constant temperature difference between the reference furnace temperature and the temperature measured at the exhausts. This temperature was measured with an insulated welded thermocouple without plate an insulation protection. This explains the oscillating registry.

3 NUMERICAL SIMULATION

The numerical simulations were performed with Fluent software, using the finite volume method, [4]. The generalized Eddy Dissipation Model was used to simulate the combustion of propane-air mixture. This model is based on the assumption that chemical reaction is almost instantaneous, when compared with the chemical species flow transportation. The combustion was modelled using a global one-step reaction mechanism, assuming complete conversion of the propane to the product species of equation 3.

$$C_3H_8 + 5\,O_2 \rightarrow 3\,CO_2 + 4\,H_2O \tag{3}$$

The reaction will be defined in terms of stoichiometric coefficients, formation enthalpies and parameters that control the reaction rate. The pressured based solver was used with unsteady and first order implicit formulation. The viscous model "K-Epsilon" with two equations and a standard wall function for near wall treatment was used. The surface to surface radiation model was used with computed view factors. The emissivity value for the internal wall furnace was considered equal to 0.7.
The use of constant transport properties for viscosity, thermal conductivity and mass diffusivity coefficients is acceptable because the flow is fully turbulent, see tables 1 and 2, [4]. The molecular transport properties will play a minor role compared to turbulent transport. The assumption of temperature dependent specific heat is an important key factor to predict more realistic peak flame temperature.

Table 1. Properties for propane–air misture, [4].

Specific heat	Mixing law	[J/kgK]
Conductivity	0.0454	[W/mK]
Viscosity	1.72×10^{-5}	[Kg/ms]

Table 2. Air properties, at reference temperature, 298 [K], [4].

Specific mass	1.225	[kg/m^3]
Specific heat	1006.43	[J/kgK]
Conductivity	0.0242	[W/mK]
Viscosity	1.7894×10^{-5}	[Kg/ms]

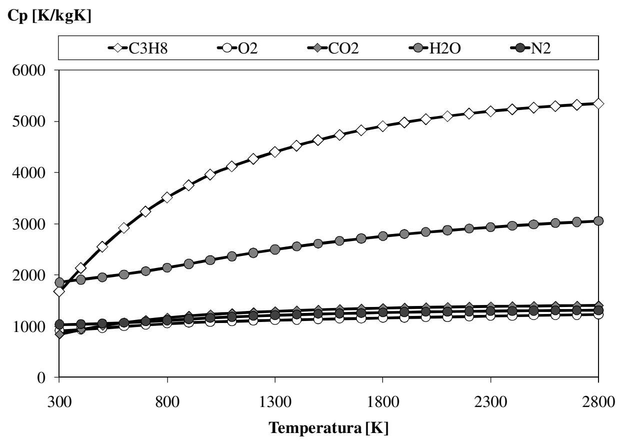

Fig.4. Variação do calor específico dos produtos e reagentes, [4].

The specific heat considered for mixture will be higher where the propane is concentrated, near the fuel inlet and where the temperature and combustion product concentration should be higher, see figure 4 for temperature dependence.
The governing equations for mass momentum and energy conservation are defined by equations 4-6.

$$\frac{\partial}{\partial t}(\rho Y_i) + \nabla \cdot (\rho \vec{v} Y_i) = -\nabla \cdot J_i + R_i \tag{4}$$

Where ρ represents the specific mass, $\vec{v}$ the velocity vector, Y_i is the local mass fraction that corresponds to the species "i", J_i the diffusion flux, while R_i represents the rate of each species formation by chemical reaction.
For the momentum conservation equation, the static pressure is defined by p, while $\bar{\bar{\tau}}$ represents the stress tensor.

$$\frac{\partial}{\partial t}(\rho \vec{v}) + \nabla \cdot (\rho \vec{v}\, \vec{v}) = -\nabla p + \nabla . \bar{\bar{\tau}} \tag{5}$$

For the energy equation, E represents the energy value, k_{eff} the effective value for conductivity, T the temperature value, h_j the sensible enthalpy, while S_h represents the energy value from chemical reaction.

$$\frac{\partial}{\partial t}(\rho E)+\nabla\cdot(\vec{v}(\rho E+p))=\nabla\cdot\left(k_{eff}\nabla T-\sum_i h_i\vec{J}_i+(\bar{\bar{\tau}}_{eff}\cdot\vec{v})\right)+S_h \tag{6}$$

An adiabatic condition was assumed in the internal furnace walls. The inlet thermal conditions were specified at room temperature. The exhaust temperature products were defined with information from experimental measured data.

The time dependence inlet velocity for air and propane were kept in proper ratio, during each test. Those values were defined according to the manufacturer limiting values, because they were not measured.

To solve the unsteady solution, the initial conditions were defined and an incremental time step was specified. An iterative process was used to solve discretized equations.

The numerical model was built with a structured mesh, using 125840 hexahedra finite volumes, each with 0.02[m] length side, see figure 5. Major simplification was introduced into the four burners, using the hydraulic diameter as reference value. Four inlet gas zones were defined concentric with the same number of air inlet zones, with dimension equal to 20x20 [mm] and 60x60 [mm], respectively. The exhaust is well identified at the bottom of the furnace volume, with rectangular dimensions equal to 100 x 400 [mm].

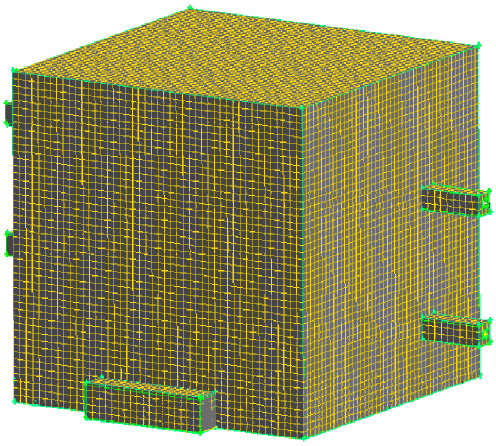

a) Finite volume mesh.

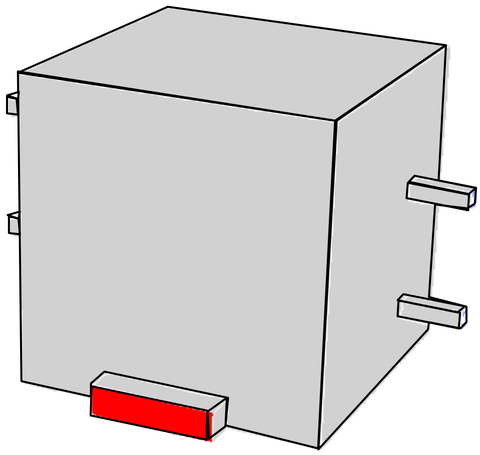

b) Solid Model, with 4 burners and exhausts.

Fig.5. Model for fire-resistance furnace.

Flame temperature depends on several factors during the combustion process and affects, significantly, heat transfer inside fire-resistance furnace. The rate of heat transfer increase with flame temperature. Figure 6 represents temperature and velocity, during the simulation of test 1, in different defined planes, in particular X150, X850, Z150, Z850 and exhaust. The burner B3/B4 plane is also represented.

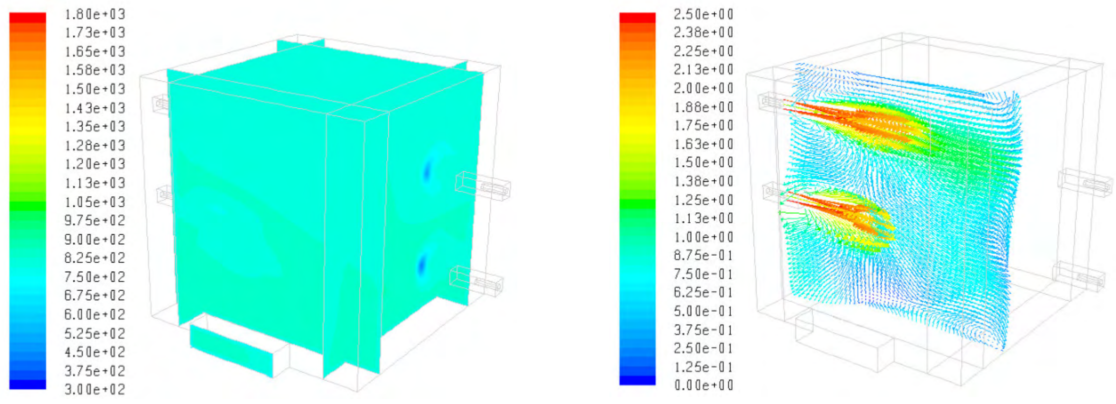

a) Contours of temperature [K] in the four planes, time =300 [s]. *b) Vector velocity in plane for burner B3/B4, time =300 [s].*

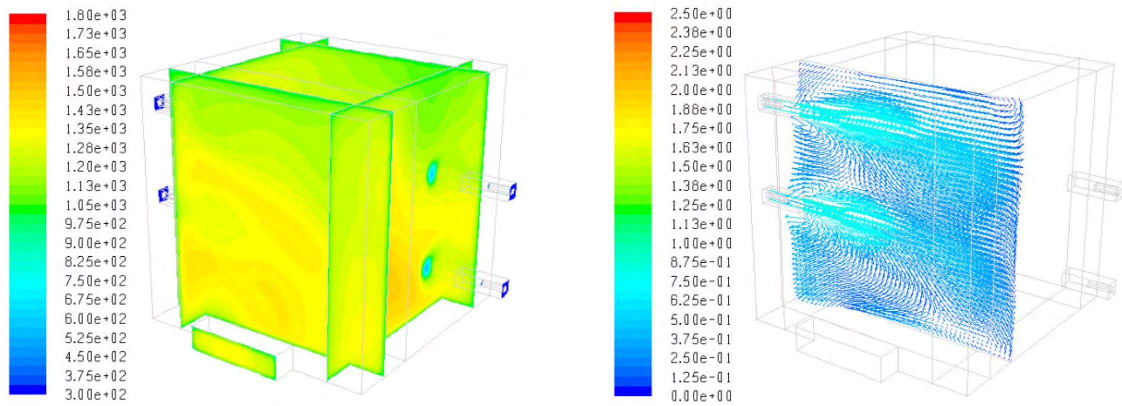

c) Contours of temperature [K] in the four planes, time =3600 [s]. *d) Vector velocity in plane for burner B3/B4, time =3600 [s].*

Fig.6. Numerical results for Test 1.

The flux of species is descendent, with small vortices zones, as can be seen in figure 6b) and d). The numerical results allow identifying the localized effect of each burner. The experimental measurements corroborate this evidence.

To determine the thermal performance of the numerical simulation, the mass average temperature value was determined for each plane defined for experiments, using equation (7). This average value is also compared with the reference value of the fire-resistance furnace, determining the relative difference, see figure 7.

$$\bar{T} = \int_A T\,\rho\,\vec{v}\,d\vec{A} \Big/ \int_A \rho\,\vec{v}\,d\vec{A} \tag{7}$$

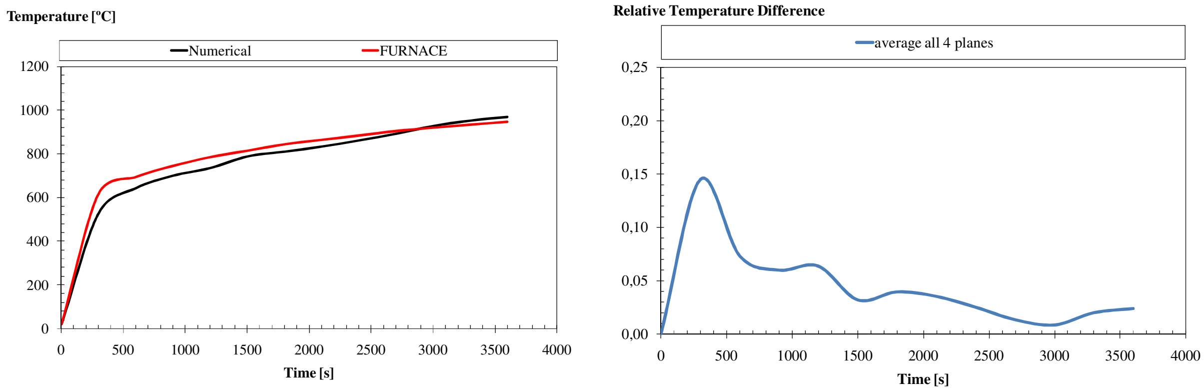

a) Numerical results, using nominal testing curve ISO834 (test1/2).

b) Relative temperature difference.

Fig.7. Average temperature value inside furnace and relative temperature difference.

The numerical results for average temperature prediction inside furnace are close to the reference temperature value for condition test 1/2, being the relative difference smaller than 10 % after 500 [s]. Besides all the thermal losses associated with this combustion process, an important loss is associated with the combustion products on exhaust. This is dependent on the species volume, temperature and also on sensible and latent heat contained in water vapour.

4 CONCLUSIONS

Three experimental tests were conducted and measurements made in four representative plans to establish the thermal performance inside the fire-resistance furnace. A comparison was made on the average of temperature measurements with the reference value. The mean deviation of the temperature in the four plans is less than 5%, for time instant greater than 500 [s]. The maximum deviation of 30% was briefly addressed at 60 [s]. In any case, the deviation of temperature is below 50 [° C]. These results validate the operating conditions of the fire-resistance furnace, and we may assume a nearly uniform distribution of temperature, for each instant of time, during tests, for both nominal fire curves.

The numerical results overestimate the value of the average temperature of the four planes under consideration. This difference may be related to the operating system conditions. To validate the numerical procedure, measurements of the instantaneous inlet air and gas flow should be performed. Additional measurements for species concentrations in the furnace exhaust should be planned for future work.

ACKNOWLEDGMENT

The authors acknowledge the financial support from the Portuguese Science and Technology Foundation, under the reference project PTDC/EME-PME/64913/2006.

REFERENCES

1. AENOR, Norma UNE 1363: Fire resistance test. Part 1: General requirements, 2000.
2. AENOR, Norma UNE 1363: Fire resistance test. Part 2: Alternative and additional procedures, October 2000.
3. S.Welch, pa Rubini. “Three dimensional simulation of a fire resistance furnace”, Proceedings of 5th International Symposium on Fire Safety Science, Melbourne, Australia, ISBN 4-9900625-5-5 International Association for Fire Safety Science (IAFSS), pp1009-1020, March 1997.
4. FLUENT 6.3 Documentation, users manual, 2006.
5. Giuliano Gardolinski Venson, Gilberto Augusto Amado Moreira, José Eduardo Mautone Barros, Ramón Molina Valle. “Modelagem do Perfil de Temperatura em Câmara de Combustão Tubular Utilizando o Modelo de Combustão Eddy Dissipation”, *X Encontro de Modelagem Computacional,* Instituto Politécnico/UERJ - Nova Friburgo/RJ, 21 a 23 de Novembro 2007.
6. Coelho, P. J. “Numerical simulation of a mild combustion burner”, Combustion and flame, 124: 503-518, Elsevier, 2001.
7. Welch, S; Rubini, P.; “Three dimensional simulation of a fire-resistance furnace”, Proceedings of 5th International Symposium on Fire Safety Science, Melbourne, Australia, March 1997, International Association for Fire Safety Science, pp. 1009-1020, ISBN 4-9900625-5-5